

# Energy dependence of strangeness production and event-by-event fluctuations

Anar Rustamov<sup>1,2,3,4,5,\*</sup>

<sup>1</sup>GSI Helmholtzzentrum für Schwerionenforschung, Darmstadt, Germany

<sup>2</sup>Physikalisches Institut, Universität Heidelberg, Heidelberg, Germany

<sup>3</sup>Baku State University, Baku, Azerbaijan

<sup>4</sup>National Nuclear Research Center, Baku, Azerbaijan

<sup>5</sup>Joint Institute for Nuclear Research, Dubna, Russia

## Abstract.

We review the energy dependence of strangeness production in nucleus-nucleus collisions and contrast it with the experimental observations in pp and p-A collisions at LHC energies as a function of the charged particle multiplicities. For the high multiplicity final states the results from pp and p-Pb reactions systematically approach the values obtained from Pb-Pb collisions. In statistical models this implies an approach to the thermodynamic limit, where differences of mean multiplicities between various formalisms, such as Canonical and Grand Canonical Ensembles, vanish. Furthermore, we report on event-by-event net-proton fluctuations as measured by STAR at RHIC/BNL and by ALICE at LHC/CERN and discuss various non-dynamical contributions to these measurements, which should be properly subtracted before comparison to theoretical calculations on dynamical net-baryon fluctuations.

## 1 Strangeness enhancement

The production of strange particles has always been at the focus of high energy nucleus-nucleus collisions. The enhancement of strange quark production, relative to light  $u$  and  $d$  quarks, in heavy-ion collisions, normalized to the corresponding signals from elementary reactions has been among the first signals for probing the Quark Gluon Plasma (QGP) formation. Indeed, in QGP, the production of a strange-antistrange quark pair can proceed by the fusion of two gluons or massless light quarks;  $q + \bar{q} \leftrightarrow s + \bar{s}$ ,  $g + g \leftrightarrow s + \bar{s}$ , with  $q$  denoting  $u$  and  $d$  quarks. For the latter only the mass excess of  $Q_{QGP} = 2m_s \approx 200$  MeV is needed. Moreover, in QGP the equilibration of strangeness is more efficient due to a large gluon density. In hadronic gas (HG), on the other hand, strangeness production proceeds in free space via e.g. associated production channels  $N + N \rightarrow N + \Lambda + K$ , with a considerably larger  $Q$  value of  $Q_{HG} = m_\Lambda + m_K - m_N \approx 670$  MeV. Based on these considerations it was advocated that strangeness production should be significantly enhanced in QGP relative to that of a free hadron gas [1–3]. Furthermore, the enhancement was predicted to depend on the strangeness content of the (anti-)baryons and to appear in a typical hierarchy;  $E_\Lambda < E_\Xi < E_\Omega$ . The enhancement,

\*e-mail: a.rustamov@cern.ch

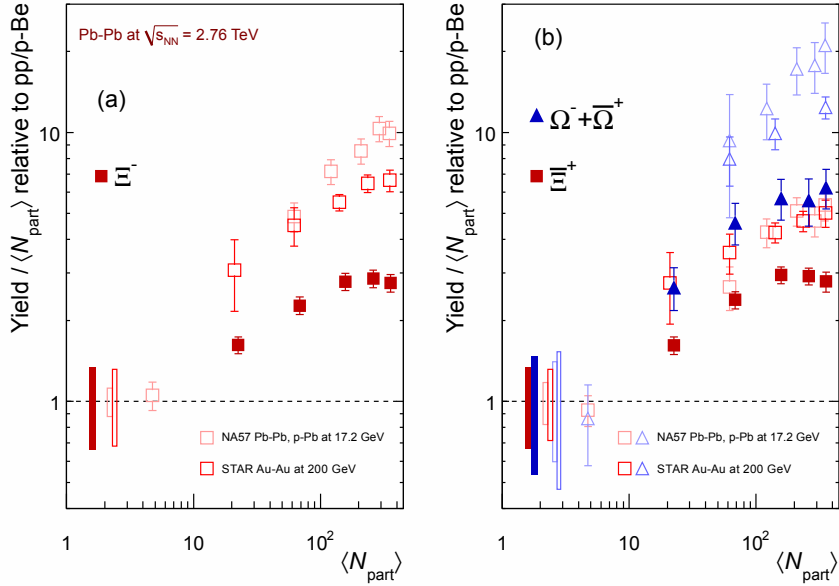


**Figure 1.** Strangeness enhancements at LHC(ALICE, full symbols), RHIC and SPS (open symbols) in the rapidity range  $|y| < 0.5$  as a function of the mean number of participant nucleons  $\langle N_{part} \rangle$ . Boxes on the dashed line at unity indicate statistical and systematic uncertainties on the pp or p-Be reference. Error bars on the data points represent the corresponding uncertainties for all the heavy-ion measurements and those for p-Pb at the SPS. For more details cf. [4] and references therein.

more in particular its predicted hierarchy, was observed experimentally as presented in the right panel of Figure 1, where it is quantified as the yield of strange particles measured in A-A collisions, per mean number of participants,  $\langle N \rangle_{part}$ , relative to pp or p-A reactions. In the case of pp reference the enhancement is therefore defined as:

$$E = \frac{Yield_{(A-A)}}{Yield_{(pp)}} \frac{2}{\langle N \rangle_{part}} \quad (1)$$

Intuitively the above prescription suggests an increase of the enhancement with increasing energy of colliding nuclei, which is at odds with the experimental measurements presented in Figure 1.

### 1.1 Strangeness suppression as apparent enhancement

As discussed in the previous section the production of strange hadrons appears to be quite different in pp reactions compared to heavy-ion collisions. This is in particular the case at low energies. The remarkable success of statistical approach in describing the hadron yields produced in nucleus-nucleus collisions clearly indicates that for a large statistical systems the conservation laws can be treated within a Grand Canonical Ensemble (GCE) formulation of statistical mechanics [5]. In this approach all hadron multiplicities are proportional to the system volume. For a small systems, however, with small (anti-)strange particle multiplicities, Canonical Ensemble (CE) have to be exploited, in which the conservation of strangeness is implemented in each micro state, i.e. on an event-by-event basis [6].

As a consequence the mean multiplicities of strange particles in CE decrease faster with decreasing volume compared to corresponding multiplicities in GCE, which means that the denominator in Eq. 1 becomes smaller due to local conservation of strangeness in smaller systems. Hence, the apparent enhancement observed experimentally is an artefact of canonical suppression in small systems, which are used as a baseline. Quantitatively it was demonstrated that, for a small values of  $x$ , with a good accuracy the canonical multiplicities are suppressed by a factor of  $F = I_s(x)/I_0(x)$  with respect to the corresponding Grand Canonical values [7, 8]. Here  $I_s(x)$  denotes the modified Bessel functions with order  $s$  and argument  $x$  is proportional to the volume of the system. This implies a number of important predictions: (i) as the strangeness content of a hadron enters into suppression factor  $F$  as an order of the Bessel function, for a fixed value of  $x$ , the larger the strangeness content the smaller the suppression factor and hence the larger the enhancement. (ii) the suppression factor decreases with decreasing energy which leads to apparent increasing trend of the enhancement with decreasing energy and (iii) for large particle multiplicities the thermodynamic limit should be reached where the suppression factor approaches unity and the differences between CE and GCE multiplicities diminish. These predictions are consistent with the experimental observations plotted in Figure 1. To shed more light on this, we present in Figure 2 the yields of  $K_s^0$ ,  $\Lambda$ ,  $\Xi$  and  $\Omega$  normalized to the pion ( $\pi^+ + \pi^-$ ) yield as a function of  $dN_{ch}/d\eta$  for various systems measured by the ALICE collaboration [9]. A significant enhancement of strange to non-strange hadron production is observed with increasing particle multiplicity in pp collisions. Moreover, the behaviour in pp and p-Pb results, albeit the latter measured at slightly lower center-of-mass energy, are consistent in terms of both the values of the ratios and their evolutions with multiplicity. At high multiplicities, the yield ratios in pp and p-Pb collisions reach values observed in Pb-Pb collisions, thus approaching the GCE limit. This observation is in line with the canonical

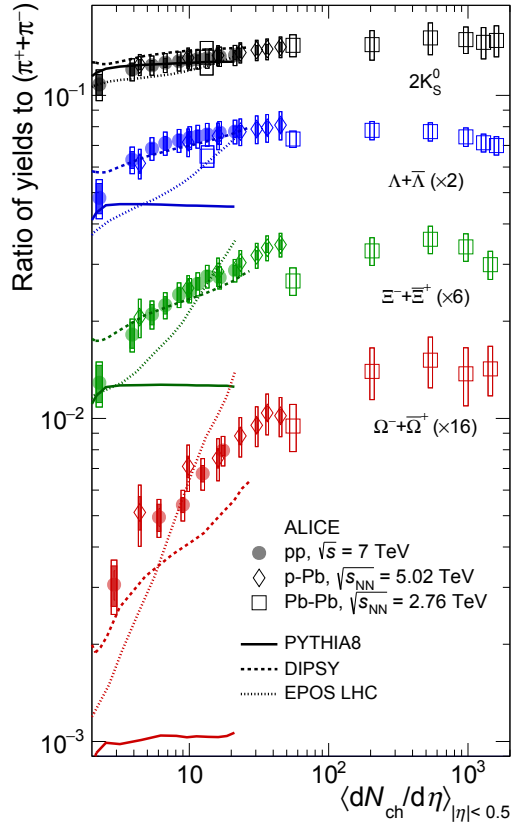


**Figure 2.** pT-integrated yield ratios to pions as a function of  $\langle dN_{ch}/d\eta \rangle$  measured in  $|y| < 0.5$ . The error bars show the statistical uncertainty, whereas the empty and dark-shaded boxes show the total systematic uncertainty and the contribution uncorrelated across multiplicity bins, respectively. The values are compared to calculations from MC models and to results obtained in p-Pb and Pb-Pb collisions at the LHC. The indicated uncertainties all represent standard deviations. For more details cf. [9] and references therein.

strangeness suppression picture and shows that the origin of the strangeness enhancement is indeed driven by the final state multiplicities rather than by the collision system and/or energy. We note that the concept of canonical strangeness suppression does not apply for a strangeness neutral  $\phi$  meson. Nonetheless, experimental results for a  $\phi$  meson also exhibit an enhancement as a function of event multiplicity (cf. Ref. [10]), i.e., it behaves like a particle with the finite net-strangeness.

## 2 Event-by-Event net-proton fluctuations

Perhaps the most challenging problem in our understanding of strongly interacting nuclear matter is its phase structure and possible existence of a critical point, at which matter undergoes a second-order phase transition. At the BNL/RHIC and CERN/SPS substantial experimental efforts are devoted to searches for a QCD critical point in ultra-relativistic heavy-ion collisions. This also serves as a motivation for the research programs at the future facilities, such as FAIR in Darmstadt and NICA in Dubna. Phase transitions can be addressed by investigating the response of the system to external perturbations via fluctuations of conserved charges. Moreover, one of the crucial issues is to establish the relation between freeze-out and the QCD chiral transition at vanishing net-baryon densities. This makes fluctuation studies at LHC of particular importance, especially in view of the reliable theoretical calculations in lattice QCD for vanishing values of baryon chemical potential [11–14]. Although LQCD predicts a Skellam behaviour for the second cumulants of net-baryon distributions at a pseudo-critical temperature of about 155 MeV, this is not the case for higher cumulants. Even on the level of second cumulants differences between HRG and LQCD results are significant for the ratio of off-diagonal susceptibilities [13, 14]. At this point we remind that, fluctuations of conserved charges are predicted in the Grand Canonical Ensemble formulation of thermodynamics [15]. In order to compare theoretical calculations within GCE, such as the Hadron Resonance Gas (HRG) model [16] and Lattice QCD (LQCD) [11], to experimental results, the requirements of GCE have to be achieved in experiments. This is typically done by analysing the experimental data in a finite acceptance by imposing cuts on rapidity and/or transverse momentum of detected particles. However, if the selected acceptance window is too small, the possible dynamical correlations we are after will also be strongly reduced [17] and consequently, net-baryons will be distributed according to the difference of two independent Poisson distributions [18]. We remind that for the Poisson distribution, all its cumulants are equal to its mean. The probability distribution of the difference  $X_1 - X_2$  of two random variables, each generated from statistically independent Poisson distributions, is called the Skellam distribution. According to the additivity of cumulants, the cumulants of the Skellam distribution will then be  $\kappa_n(\text{Skellam}) = \langle X_1 \rangle + (-1)^n \langle X_2 \rangle$ , where  $\langle X_1 \rangle$  and  $\langle X_2 \rangle$  are mean values of  $X_1$  and  $X_2$  respectively. On the other hand, the increase of the acceptance will enlarge significance of correlations due to baryon number conservation. In order to be more sensitive to dynamical fluctuations, the better approach is to study the fluctuation of conserved charges in a larger acceptance and subtract the correlation part caused by the global conservation laws. This is actually the appropriate way to address the fluctuation physics when both, trivial and dynamical fluctuations are close to Poisson probability distributions. To proceed further we provide the necessary definitions. The first four cumulants of net-baryon  $\Delta n_B = n_B - n_{\bar{B}}$  distribution are defined as:

$$\begin{aligned}
 \kappa_1(\Delta n_B) &= \langle \Delta n_B \rangle \\
 \kappa_2(\Delta n_B) &= \langle (\Delta n_B - \langle \Delta n_B \rangle)^2 \rangle \\
 \kappa_3(\Delta n_B) &= \langle (\Delta n_B - \langle \Delta n_B \rangle)^3 \rangle \\
 \kappa_4(\Delta n_B) &= \langle (\Delta n_B - \langle \Delta n_B \rangle)^4 \rangle - 3\kappa_2^2(\Delta n_B)
 \end{aligned}
 \tag{2}$$

The second cumulant can be represented as a sum of corresponding cumulants for single baryons plus the correlation term for joint probability distributions of baryons and antibaryons

$$\kappa_2(\Delta n_B) = \kappa_2(n_B) + \kappa_2(n_{\bar{B}}) - 2(\langle n_B n_{\bar{B}} \rangle - \langle n_B \rangle \langle n_{\bar{B}} \rangle). \quad (3)$$

Eq. 3 shows that, in the case of missing correlations between baryons and antibaryons,  $\langle n_B n_{\bar{B}} \rangle = \langle n_B \rangle \langle n_{\bar{B}} \rangle$ , the second cumulant of net-baryons is exactly equal to the sum of the corresponding second cumulants for baryons and antibaryons. A correlation can emerge, in addition to that originating from critical fluctuations, from conservation laws. If the experimental acceptance is large enough the correlation term in Eq. 3 acquires a finite value. Hence we expect that the second cumulant of net-baryons becomes smaller than the sum of baryons and antibaryons.

We note that in this work net-protons are used as a proxy for net-baryons, which is justified at higher center-of-mass energies ( $\sqrt{s_{NN}} > 10$  GeV) [19].

## 2.1 Results and discussions

Recently the ALICE collaboration reported on the second cumulants of net-proton distributions, measured in Pb-Pb collisions at  $\sqrt{s_{NN}} = 2.76$  TeV [20]. The analysis of experimental data was performed with the Identity Method [21–25]. Furthermore, based on the recently proposed model, it was demonstrated that non-dynamical fluctuations, such as those stemming from unavoidable fluctuations of participant nucleons are immaterial for the second cumulants of net-protons measured at LHC energies [18]. The obtained results for the second cumulants of net-protons, normalised to the Skellam baseline, are presented in the left panel of Figure 3. For pseudorapidity ranges of  $|\eta| < 0.4$ , which corresponds to  $\Delta\eta < 0.8$ , the experimentally measured net-proton distributions follow a Skellam distribution. This agreement is due to the small acceptance as discussed above. Beyond  $\Delta|\eta| > 0.8$ , however, some deviations from the Skellam baseline are observed. It is argued that these deviations, as a functions of acceptance, are due to the global baryon conservation, which should be corrected for before comparison to theoretical calculations within GCE. For the second cumulants the contribution from the global baryon number conservation depends only on the acceptance factor  $\alpha = \langle n_p \rangle / \langle N_B^{4\pi} \rangle$  with  $\langle n_p \rangle$  and  $\langle N_B^{4\pi} \rangle$  referring to the mean number of protons inside the acceptance and the mean number of baryons in the full phase space respectively [18]:

$$\frac{\kappa_2(p - \bar{p})}{\kappa_2(\text{Skellam})} = 1 - \alpha. \quad (4)$$

For each rapidity range the acceptance factor was then estimated using the total number of baryons as measured by the ALICE experiment in the pseudorapidity range of  $|\eta| < 0.5$  [26]. Next, from HIJING and AMPT simulations, total number was obtained of baryons in the full phase space. The number of protons, used in the definition of  $\alpha$  (cf. Eq. 4), was taken from the experimental analysis for each rapidity range. Finally, using these values of  $\alpha$  the red band in the left panel of Figure 3 was calculated with Eq. 4. The finite width of the band reflects the difference between the two event generators. We hence conclude that the reported deviation from Skellam is caused by global baryon number conservation and that other possible dynamical fluctuations are not visible in the second cumulants of net-protons measured at LHC energies.

In the right panel of Figure 3 the ratio of fourth to second cumulants,  $k\sigma^2 = \kappa_4(p - \bar{p}) / \kappa_2(p - \bar{p})$  of net-proton, proton and anti-proton for the 5% most central Au+Au collisions are presented, as measured by the STAR Collaboration. The data shows strong enhancement at lowest center-of-mass energy of 7.7 GeV, while results at 19.6, 27 and 39 GeV are below the HRG baseline. For higher energies, however, the data, within uncertainties, is consistent with unity. Moreover, the transport

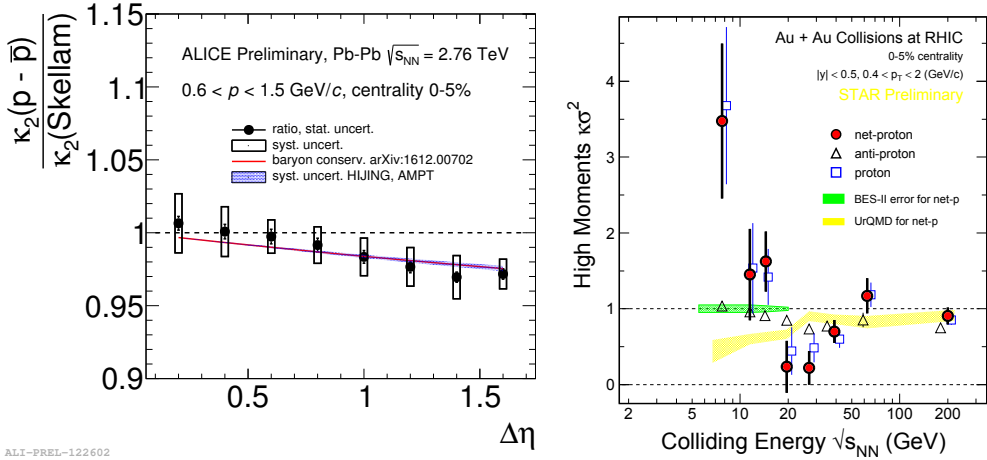


**Figure 3.** Left panel: Pseudorapidity dependence of the normalised second cumulants of net-protons as measured by the ALICE experiment at LHC. The red solid line shows the effect of the baryon number conservation. Right panel: Ratio of fourth to second cumulants as measured by the STAR Collaboration for Au+Au collisions at different center-of-mass energies.

model UrQMD exhibits smooth decrease with decreasing energy. Few comments are in order at this point; (i) in order to get rid of participant fluctuations [18, 27], the experimental data of STAR was corrected with the so called Centrality Bin Width Correction (CBWC) procedure [28, 29]. The essential idea behind the CBWC is to get rid of the participant fluctuations by subdividing a given centrality bin into smaller ones and then merging them together incoherently [30]. However, although CBWC procedure reduces the overall level of fluctuations significantly it cannot fully eliminate the participant fluctuations; (ii) the same rapidity interval of  $|y| < 0.5$  is used for all energies. This leads to significant decrease of the fraction of accepted protons with increasing energy and increases the artefacts of global baryon number conservation at low energies, which drives the results at  $\sqrt{s_{NN}} = 19.6, 27$  and  $39$  GeV below unity. This explanation is also consistent with the energy dependence of the UrQMD results. Obviously baryon number conservation cannot explain the increase observed at lower energies. Recently it was argued that independent combination of baryon stopping and participant fluctuations also cannot explain this increase, though assumption of the collective stopping of multiple baryons catches the essential part of the observed structure [31].

### 3 Conclusions

In summary we reviewed the energy dependence of so-called strangeness enhancement in A-A collisions relative to small interacting systems. We argued that originally proposed idea of the strangeness enhancements contradicts with the energy dependence of enhancement observed experimentally. On the other hand, calculations within statistical models in Canonical Ensemble indicates that the observed enhancement is in fact the artefact of strangeness suppression in small systems, which are used as a baseline to quantify the observed apparent enhancement. Although this explains nearly all measured signals, including the reported energy dependence, the procedure fails to reproduce the centrality dependence of strangeness neutral  $\phi$  meson production. In this case the canonical suppression is irrelevant, although the data indicates a suppression similar to other particles with non-zero net

strangeness. Next, we reviewed first measurements of net-proton fluctuations from the ALICE experiment at LHC and discussed preliminary results from the STAR experiment. The measured second cumulants of net-protons by the ALICE Collaboration, which are used as a proxy for net-baryons, are, after accounting for baryon number conservation, in agreement with the corresponding second cumulants of the Skellam distribution. We note that LQCD predicts a Skellam behaviour for the second cumulants of net-baryon distributions at a pseudo-critical temperature of about 155 MeV, which is very close to the freeze-out temperature from the HRG model applied to the ALICE data. Critical behaviour is predicted by LQCD starting from second off-diagonal cumulants, the analysis of which is ongoing in ALICE. The non-monotonic energy excitation of fourth to second ratio of cumulants of net-protons, reported by STAR, can be partially explained by the global baryon number conservation, while the increase of fluctuations at lower energies still to be understood. It is however expected that non-dynamical fluctuations, such as those stemming from participant fluctuations are still present in the final results, because the applied CBWC procedure cannot eliminate them entirely. There is no general consensus whether or not the observed non-monotonic energy dependence is indeed connected to the critical phenomena associated with the second order phase transition at the critical point.

## Acknowledgments

The author acknowledges stimulating discussions with Peter Braun-Munzinger. This work is part of and supported by the DFG Collaborative Research Centre "SFB 1225 (ISOQUANT)". The research was also supported in part by the ExtreMe Matter Institute EMMI at the GSI Helmholtzzentrum fuer Schwerionenphysik, Darmstadt, Germany

## References

- [1] J. Rafelski and B. Müller, *Phys. Rev. Lett.* 48 (1982) 1066.
- [2] P. Koch, J. Rafelski, and W. Greiner, *Phys. Lett. B* 123 (1983) 151.
- [3] P. Koch, B. Müller, and J. Rafelski, *Phys. Rep.* 142 (1986) 167.
- [4] ALICE Collaboration, *Phys.Lett. B*728 (2014) 216-227, Erratum: *Phys. Lett. B*734 (2014) 409-410.
- [5] J. Stachel, A. Andronic, P. Braun-Munzinger and K. Redlich, *J. Phys. Conf. Ser.* 509 (2014) 012019
- [6] M.I. Gorenstein, W. Greiner, A. Rustamov, *Phys.Lett. B*731 (2014) 302-306.
- [7] K. Redlich, A. Tounsi, *Eur.Phys.J. C*24 (2002) 589-594.
- [8] S. Hamieh, K. Redlich, A. Tounsi, *Phys.Lett. B*486 (2000) 61-66
- [9] ALICE Collaboration, *Nature Phys.* 13 (2017) 535-539.
- [10] V. Viskovic, A. Kalweit, arXiv:1610.03001.
- [11] A. Bazavov et al., *Phys. Rev. D*85 (2012) 054503.
- [12] B. Friman, F. Karsch, K. Redlich, and V. Skokov, *Eur. Phys. J. C*71 (2011) 1964.
- [13] F. Karsch, *Nucl.Phys. A*967 (2017) 461-464.
- [14] O. Kaczmarek, *Nucl.Phys. A*967 (2017) 137-144.
- [15] L. D. Landau and E. M. Lifshitz, *Statistical Physics*, Pergamon Press, 1980.
- [16] A. Andronic, P. Braun-Munzinger, K. Redlich, and J. Stachel, *J.Phys.Conf.Ser.* 779 (2017).
- [17] V. Koch, in "Relativistic Heavy Ion Physics", R. Stock (ed.) (Springer, Heidelberg, 2010), (Landolt-Boernstein New Series I, v. 23) p. 626, arXiv:0810.2520v1.
- [18] P. Braun-Munzinger, A. Rustamov, J. Stachel, *Nucl. Phys. A*960 (2017), 114.

- [19] M. Kitazawa, and M. Asakawa, Phys. Rev. C86 (2012) 024904 and erratum, ibidem 069902, arXiv:1205.3292 [nucl-th].
- [20] A. Rustamov for the ALICE Collaboration, Nucl.Phys. A967 (2017) 453-456.
- [21] M. Gazdzicki et al., Phys. Rev. C83 (2011) 054907 .
- [22] M. I. Gorenstein, Phys. Rev. C84 (2011) 024902.
- [23] A. Rustamov, M. I. Gorenstein, Phys. Rev. C86 (2012) 044906.
- [24] T. Anticic et al. (NA49 Collab.), Phys.Rev. C89 (2014) 054902.
- [25] M. Arslanok for the ALICE Collaboration, Nucl.Phys. A956 (2016) 870-873.
- [26] P. Braun-Munzinger, A. Kalweit, K. Redlich, and J. Stachel, Phys.Lett. B747 (2015) 292.
- [27] V. Skokov, B. Friman, and K. Redlich, Phys.Rev. C88 (2013) 034911.
- [28] X. Luo, PoS (CPOD2014) 019, arXiv:1503.02558.
- [29] X. Luo, N. Xu, Nucl.Sci.Tech. 28 (2017) no.8, 112.
- [30] X. Luo, J. Xu, B. Mohanty, N. Xu, J. Phys. G 40 (2013) 105104.
- [31] A. Bzdak, V. Skokov, Eur.Phys.J. C77 (2017) no.5, 288.